Much stronger binding of metal adatoms to silicene than to graphene: A first-principles study

Xianqing Lin and Jun Ni*
Department of Physics and State Key Laboratory of Low-Dimensional Quantum Physics, Tsinghua University, Beijing 100084, Peoples Republic of China
(Received 11 June 2012; published 20 August 2012)

First-principles calculations have been performed to study the structural, energetic, and electronic properties of 15 different metal atoms adsorbed on silicene. Among the 15 metal adatoms on silicene, Li, Na, K, Ca, Co, Ni, Pd, and Pt obtain a larger binding energy than the cohesive energy of the bulk metal. While the binding of Au and Sn to graphene is rather weak, they bind strongly and covalently to silicene. For the alkali metal adatoms on silicene, the bonding is approximately ideal ionic. When the Ca atom is adsorbed on silicene, hybridization between the Ca 3*d* states and the silicene states occurs around E_F besides charge transfer from Ca to silicene. The Al, Ga, In, and Sn adatoms bind most strongly at the top site above a Si atom in silicene and form strong covalent bonds with the nearest Si atoms. For the Ti, Fe, Co, and Au adatoms on silicene, the adatom *d* states are strongly hybridized with the silicene states around E_F, while the hybridization states lie rather far below the E_F with E_F located approximately at the Dirac point for the Ni, Pd, and Pt adatoms on silicene. The strong binding of metal adatoms to silicene and the rich electronic properties of the systems suggest possible experimental exploration of functionalization of silicene with metal adatoms.

DOI: 10.1103/PhysRevB.86.075440 PACS number(s): 73.22.−f, 68.43.Fg, 73.20.Hb

I. INTRODUCTION

Since the discovery of graphene in 2004,[1] this single layer carbon honeycomb structure has attracted significant interest in exploring the rich condensed-matter physical phenomena and possible ways of functionalizing graphene for potential applications.[2–5] The unique symmetry of the honeycomb π-orbital network makes graphene exhibit peculiar electronic structure. The states near the Fermi level (E_F) have zero band gap and show linear energy dispersion, suggesting the Dirac-type behavior of the motion of quasiparticles with energies near E_F in graphene.[3] Silicon and carbon belong to group IV of the periodic table. They have similar valence electron configurations with Si having a larger atomic radius and lower electronegativity. Thus the silicon materials can possess many distinct properties. The bulk silicon has a diamond-like structure with a much smaller band gap than diamond and has been the base for the microelectronics industry. While carbon atoms can form layered graphite, the graphite-like silicon allotrope does not exist. Nevertheless, much effort has been devoted to the synthesis of the graphene-like silicon two-dimensional structure,[6–11] which is referred to as silicene. Recently, silicene has been successfully synthesized on the Ag (111) surfaces, and linear energy dispersion was observed.[11] Theoretical studies have found that silicene shows great similarity of electronic structure to graphene.[12–15] On the other hand, the differences in other properties between silicene and graphene are also interesting and remain to be explored.

Besides the intriguing properties of the pristine graphene, the adsorption of metal atoms provides a variety of ways of modifying the electronic properties of graphene as well as functionalization of graphene for applications. Alkali and alkali-earth metal adatoms can dope electrons into graphene.[16] Superconductivity may be realized in Li-coated graphene with a relatively high critical temperature (T_c).[17] The graphene sheets adsorbed with some metal atoms are predicted to be promising host materials for hydrogen storage.[18–21] Some transition metal atoms doped in graphene may act as catalysts for certain chemical reactions.[22,23] For applications in hydrogen storage and superconductivity, high coverage of metal adatoms on graphene is required. In order to improve the performance of possible catalytic metal adatoms, the adatoms may be requested to remain isolated rather than forming three dimensional (3D) clusters. However, because the binding energies (E_b) of all studied metal adatoms on graphene are smaller than the cohesive energies (E_c) of the bulk metals,[16,24,25] clustering is probably inevitable when depositing metal atoms on graphene with high coverage.[26] In order to achieve larger E_b of metal atoms in graphene than E_c, some metal atoms are proposed to substitute the carbon atoms in graphene.[27] For substitution of carbon in graphene by metal atoms, vacancies have to be created first using a highly focused electron beam, which will also cause severe damage to the structure of graphene.[28] Compared with graphene, the hexagons in silicene have a larger size. And silicene is stable as a buckled sheet with the two sublattices not in the same plane. Moreover, the Si-Si bonds in silicene acquire partial sp^3 characteristics rather than complete sp^2 hybridization in graphene.[29] Therefore, silicene provides different structural and electronic circumstances from graphene for interaction of metal adatoms with the neighboring Si atoms. It is worth searching for metal adatoms on silicene which obtain larger E_b than E_c or exhibit different electronic properties from graphene.

In this work, we have systematically investigated the structural, energetic, and electronic properties of 15 different metal atoms adsorbed on silicene using first-principles calculations, including alkali and alkali-earth metals, groups III and IV metals, and transition metals. We find that among the 15 metal adatoms on silicene, Li, Na, K, Ca, Co, Ni, Pd, and Pt obtain a larger E_b than E_c. The Al, Ga, and In adatoms form covalent bonds with their nearest Si atoms rather than bond ionically to the substrate as on graphene. While the interaction of the Au and Sn adatoms with graphene is rather weak,[16] they bind strongly and covalently to silicene.

The outline of this paper is as follows: Section II describes the calculation details. In Sec. III, we show the structural, energetic, and electronic properties of alkali and alkali-earth metal adatoms, groups III and IV metal adatoms, and transition metal adatoms on silicene, respectively. Section IV is the summary.

II. METHODS

The spin-polarized DFT is employed in our electronic structure calculations using the VASP code.[30] The generalized gradient approximation (GGA) with the Perdew-Burke-Ernzerhof (PBE) exchange-correlation functional[31] is adopted. The projector augmented wave (PAW) potentials[32] are used with a kinetic energy cutoff of 520 eV. For the silicene unit cell, the Brillouin zone (BZ) sampling is done using a $24 \times 24 \times 1$ Monkhorst-Pack grid[33] for relaxation calculations and a $40 \times 40 \times 1$ Monkhorst-Pack grid for static calculations. The Monkhorst-Pack grid for a silicene supercell is chosen to be inversely proportional to the dimensions of the supercell. We represent the direction perpendicular to the silicene plane as the z direction. The vacuums in the z direction are larger than 16 Å. The tolerance for the energy convergence is 10^{-5} eV. All structures are fully relaxed until the force on each atom is smaller than 0.01 eV/Å. For metal adatoms bonding ionically with silicene, there exists spurious interaction between the dipole moments of the periodic images in the z direction. So the dipole corrections implemented in the VASP code[34,35] are applied to the potential and total energy in the cases with ionic bonding.

In contrast to the planar sheet of graphene, silicene has a buckled hexagonal structure, as shown in Fig. 1. The relaxed silicene unit cell has a lattice constant of 3.87 Å, which is 2.47 Å for the graphene unit cell.[16] The buckled height between the two Si atoms in the unit cell is 0.46 Å. Then the two sublattices of silicene are naturally distinguished from each other by their positions in the z direction. We denote the sublattice with a smaller z coordinate as sublattice A. The other sublattice is denoted as sublattice B.

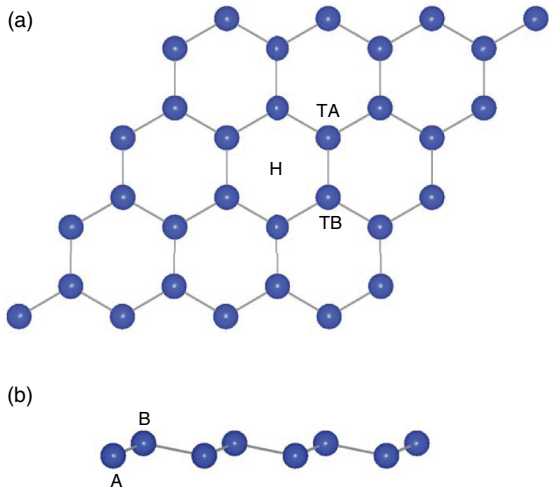

FIG. 1. (Color online) (a) and (b) The buckled hexagonal structure of silicene. The three adsorption sites considered H, TA, and TB are indicated in (a). The sublattices A and B are labeled in (b).

A supercell consisting of 4×4 silicene unit cells is employed for the adsorption of metal atoms on silicene. The distance between the neighboring metal adatoms is 15.46 Å, which is 9.88 Å for the 4×4 graphene supercell.[16] Thus the interaction between metal adatoms is rather weak so that the systems with a metal adatom on the 4×4 silicene supercell can be considered to be an approximation of the interaction between an isolated adatom with silicene. For the 4×4 silicene supercell with metal adatoms, the density of states (DOS) is calculated using a refined $24 \times 24 \times 1$ Monkhorst-Pack grid together with the Gaussian smearing method with the broadening width equal to 0.1 eV. The partial DOS (PDOS) is calculated by projecting the wave functions onto spherical harmonics within a sphere around each atom, and the sum of the PDOS of each atom is thus in general not equal to the calculated total DOS. The PDOS can represent the contribution of an atomic orbital to the electronic states qualitatively.

We consider three different adsorption sites: the hollow (H) site above the center of a hexagon, the top (TA) site above a Si atom of sublattice A, and the top (TB) site above a Si atom of sublattice B. When the metal atoms are placed above the midpoint of a Si-Si bond (bridge site), all the adatoms are found to be at the TA site after structural relaxations. We denote a metal adatom on silicene as M. For all the M-silicene systems, we define the binding energy of M on silicene as

$$E_b(\mathrm{M}) = E(\mathrm{M}) + E(\mathrm{Silicene}) - E(\mathrm{M\text{-}Silicene}),$$

where E(M), E(Silicene), and E(M-Silicene) are the energies of an isolated metal atom, the silicene supercell, and the adatom-silicene system. The larger E_b, the stronger the binding of the metal adatom to silicene.

III. RESULTS

A. Alkali and alkali-earth metal adatoms

We first consider the adsorption of the Li, Na, K, and Ca atoms on silicene. All four adatoms bind most strongly to the H site with E_b larger than the cohesive energy (E_c) per atom in the corresponding bulk metals.[36] The K adatom on silicene has the largest ratio of E_b to E_c (E_b/E_c), which reaches 2.040. For metal adatoms on graphene, K also has the largest E_b/E_c of 0.859, smaller than 1.000. Similar to alkali metal adatoms on graphene,[16] the bonding between Li, Na, and K and silicene is ionic. The s states of these adatoms are all empty and lie rather far above E_F. Thus about one electron (e) of charge per adatom is transferred from the alkali metal adatoms to silicene, and the adatoms have no local magnetic moments. In contrast, the Na and K atoms adsorbed on graphene are magnetic, with the spin-up s states of the adatoms lying close to E_F.[16] While the Ca adatom bonds ionically with graphene, hybridization between the Ca $3d$ states and the silicene states occurs around and above E_F, leading to partial covalent bonding between Ca and silicene.

The binding energies of all the considered metal adatoms at the three sites of silicene as well as the geometrical parameters are given in Table I. The Li, Na, K, and Ca adatoms on silicene have the largest E_b at the H site and the smallest E_b at the TB site. The E_b of these adatoms at the H site are all larger than E_c. Among the alkali metal adatoms at the H site, Li binds

TABLE I. The binding energies of all metal adatoms considered here at the three adsorption sites of silicene as well as the geometrical parameters: the binding energy of adatoms on silicene (E_b), the binding energy of adatoms on graphene ($E_{b,\text{graphene}}$) calculated within the GGA from Ref. 23 (Co, Ni), Ref. 24 (Pt), and Ref. 16 (other adatoms), the experimental value of the cohesive energy per atom in the bulk metal (E_c) from Ref. 33, the ratio of E_b to E_c (E_b/E_c), the height of the adatom over the plane of sublattice B defined by the farthest Si atom, the bond length between the adatom and its nearest Si atoms ($d_{\text{M-Si}}$), the differences between the largest and smallest z coordinates of Si atoms in sublattice A (Δz_A) and sublattice B (Δz_B).

Atom	Site	E_b (eV)	E_c (eV)	E_b/E_c	$E_{b,\text{graphene}}$ (eV)	h (Å)	$d_{\text{M-Si}}$ (Å)	Δz_A (Å)	Δz_B (Å)
	H	2.129	1.630	1.306	1.096	1.21	2.72	0.34	0.45
Li	TA	1.896				1.77	2.61	0.43	0.05
	TB	1.718				1.42	2.58	0.15	1.28
	H	1.613	1.113	1.449	0.462	1.79	3.06	0.28	0.39
Na	TA	1.468				2.23	2.94	0.26	0.06
	TB	1.325				2.10	2.81	0.09	0.74
	H	1.905	0.934	2.040	0.802	2.40	3.46	0.23	0.32
K	TA	1.799				2.46	3.41	0.52	0.33
	TB	1.704				2.52	3.18	0.19	0.68
	H	2.188	1.840	1.189	0.632	1.69	2.91	0.33	0.31
Ca	TA	2.159				1.82	2.90	1.00	0.20
	TB	2.125				1.35	3.01	0.57	2.02
	H	2.494				1.69	2.78	0.43	0.18
Al	TA	2.828	3.390	0.834	1.042	1.57	2.55	1.07	0.07
	TB	2.717				1.48	2.53	0.41	1.61
	H	2.305				1.86	2.89	0.24	0.11
Ga	TA	2.397	2.810	0.853	0.858	1.70	2.63	1.01	0.09
	TB	2.261				1.58	2.59	0.39	1.58
	H	2.006				1.95	3.07	0.34	0.29
In	TA	2.138	2.520	0.848	0.690	2.03	2.95	0.78	0.10
	TB	1.951				1.87	2.91	0.30	1.49
	H	2.458				1.56	2.81	0.65	0.44
Sn	TA	2.937	3.140	0.935	0.256	1.67	2.75	0.87	0.14
	TB	2.844				1.70	2.74	0.38	1.46
	H	3.899	4.850	0.804	1.869	1.00	2.50	0.51	0.30
Ti	TA	3.832				1.56	2.48	0.68	0.30
	TB	3.646				1.75	2.48	0.90	1.08
	H	3.430				-0.33	2.30	0.28	0.22
Fe	TA	3.516	4.280	0.821	0.748	1.16	2.28	0.93	0.11
	TB	3.374				1.11	2.28	0.49	1.46
	H	4.463	4.390	1.017	2.080	0.28	2.27	0.57	0.41
Co	TA	4.058				1.02	2.29	1.03	0.22
	TB	3.934				0.90	2.29	0.23	1.70
	H	4.776	4.440	1.076	2.790	0.27	2.31	0.50	0.49
Ni	TA	4.169				0.97	2.25	0.96	0.22
	TB	3.963				0.97	2.24	0.30	1.52
	H	4.200	3.890	1.080	1.081	0.60	2.46	0.43	0.47
Pd	TA	3.701				1.30	2.42	0.83	0.23
	TB	3.493				1.09	2.42	0.23	1.64
	H	5.871	5.840	1.005	2.170	0.43	2.42	0.50	0.56
Pt	TA	5.248				1.14	2.41	0.94	0.25
	TB	5.130				0.98	2.43	0.23	1.76
	H	2.316	3.810	0.608	0.096	1.01	2.56	0.38	0.38
Au	TA	2.159				1.30	2.56	1.14	0.33
	TB	1.977				1.22	2.57	0.25	1.74

most strongly to silicene and has the smallest height (h) over the silicene plane of 1.21 Å. The increasing of h from the Li to K adatoms is due to the increasing atomic radius. When the Li atom is adsorbed on graphene, the h is as large as 1.71 Å.[16] The much smaller h of Li on silicene than on graphene is mainly due to the larger dimension of the hexagon in silicene than that in graphene.

Since silicene has been experimentally grown on the Ag (111) surface,[11] we have also considered the adsorption of the K atom on silicene supported by the Ag (111) surface. We use

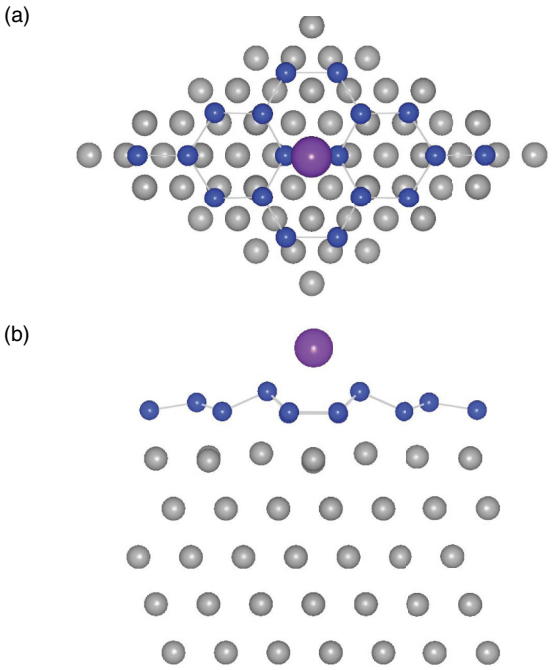

FIG. 2. (Color online) (a) and (b) The relaxed structure for the K adatom at the bridge site of silicene supported by the Ag (111) surface. The gray circles represent the Ag atoms, the smaller dark circles represent the Si atoms, and the larger dark circle represents the K atom.

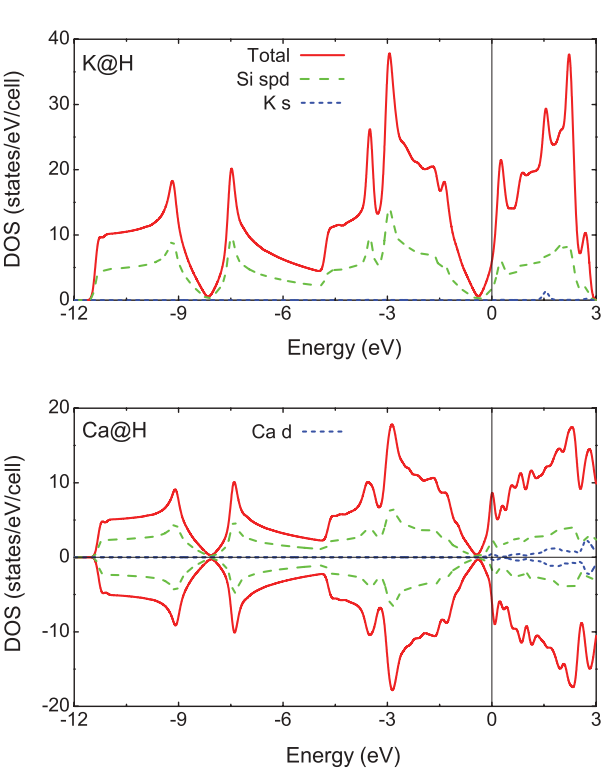

FIG. 3. (Color online) (a) The total DOS, PDOS from the silicene states, and PDOS from the K s state for the K adatom at the H site (K@H) on silicene. The solid and dashed lines represent the total DOS and PDOS from the silicene states for all the DOS plots in this work. The PDOS from the K s state is multiplied by 4.0 and is represented by the short dashed line. The energy is relative to E_F for all the DOS plots. (b) The DOS plots for Ca@H on silicene. The up and down panels show the DOS for the spin-up and spin-down states, respectively.

the structure of silicene on the Ag (111) surface observed by P. Vogt *et al*. in experiments.[11] The 3×3 silicene supercell is placed on the 4×4 supercell of the Ag (111) surface. The silicene sheet on the Ag (111) surface is also buckled with a buckled height of 0.77 Å, which is consistent with the results calculated by P. Vogt *et al*.[11] We have considered all the possible hollow, top, and bridge sites. We find that the K adatom binds most strongly to the bridge site above the Si-Si bond connecting the buckled hexagon, as shown in Fig. 2. The E_b of the K adatom at the bridge site of silicene on the Ag (111) surface is 2.142 eV, as large as that of the K atom adsorbed at the H site of the pristine silicene, and is thus larger than E_c. The height of the K adatom over the highest Si atoms with respect to the Ag (111) surface is 2.10 Å. The K-Si bond length is 3.38 Å, a little smaller than that for K at the H site of the pristine silicene. In addition, we have calculated the diffusion barrier of the K atom adsorbed on the pristine silicene. For the K adatom on graphene, K. T. Chan *et al*. estimated the diffusion barrier as the difference between the E_b at the hollow and bridge sites, which is 0.063 eV.[16] For the K atom adsorbed on silicene, the difference between the E_b at the H and TA sites is 0.106 eV, larger than the estimated diffusion barrier of the K adatom on graphene. Moreover, we have calculated the energy barrier for the diffusion of the K adatom on silicene from the H to TA site using the nudged elastic band (NEB) method,[37] which is about 0.108 eV, almost equal to the difference between the E_b at the H and TA sites. We have also considered the direct migration of the K adatom between the neighboring H sites through the top of the Si-Si bond. The calculated diffusion barrier using the NEB method is 0.196 eV. Therefore, the K adatom on silicene favors the diffusion path from the H to TA site, then to the next H site. In addition, as a result of the charge transfer from the K adatoms to silicene, the K adatoms are positively charged. It is noted that the well ordered K layer on graphite[16,38] and Cs layer on graphene[39] have been realized in experiments. For the K adatoms on silicene, the E_b is larger than E_c, the diffusion barrier is a little larger than that of the K adatom on graphene and there exists repulsive interaction between the positively charged K adatoms. It is thus worth exploring experimentally the possibility of the formation of the K layer on silicene.

The DOS for the K adatom at the H site (K@H) and Ca@H on silicene are shown in Fig. 3. For K@H, the electronic states of silicene remain almost unaltered compared with the pristine silicene except for the charge transfer from K to silicene. Thus E_F is shifted above the Dirac point. The energy of the Dirac point is denoted as E_D. The energy difference between E_F and E_D is approximately the same for the Li, Na, and K adatoms on silicene and is about 0.39 eV. This indicates that almost the same amount of charge is transferred from a Li, Na, and K adatom to silicene. By integrating the total DOS from E_D to E_F, we find that about 1.00 electron of charge per adatom is transferred to silicene. In addition, we note that the K 4s peak lies 1.56 eV above E_F and is thus totally empty. Moreover, there is no significant peak for the DOS of Si atoms around the K 4s peak. The positions of the adatom s peaks relative to E_F

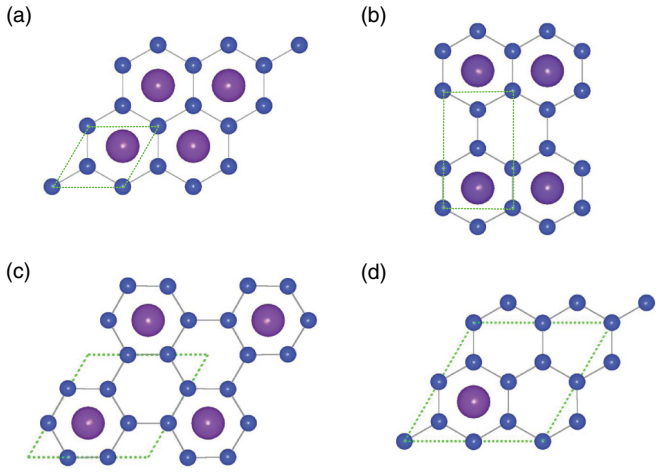

FIG. 4. (Color online) The structure models of alkali and alkali-earth metal adatoms on silicene with coverage $\theta = 1$ (a), $\theta = 1/2$ (b), $\theta = 1/3$ (c), and $\theta = 1/4$ (d). The dotted line shows the unit cell for each structure.

for Li and Na are 1.85 and 1.46 eV, respectively. In contrast, the spin-up 4s peak of K on graphene is partially occupied so that the charge transfer from a K adatom to graphene is smaller than 1.0 e.[16] When Ca is adsorbed at the H site of silicene, hybridization between the 3d states of Ca and the silicene states occurs around and above E_F. Nevertheless, the Dirac point is still clearly visible and is 0.44 eV below E_F. In the vicinity of and below E_D, the silicene states are unaffected by the adsorption of Ca atoms. The Ca adatom on silicene has a magnetic moment of 0.70 μ_B with an energy splitting of about 0.09 eV between the spin-up and spin-down Ca 3d peaks near E_F. The E_b for Ca adsorbed on silicene is 2.188 eV, while it is only 0.632 eV on graphene.[16] The much stronger binding of Ca to silicene than to graphene is probably due to the partial covalent bonding between the Ca adatom and silicene.

Since the Li, Na, K, and Ca adatoms on silicene have a much larger E_b than E_c, stable and ordered structures with high coverage of these adatoms on silicene can be realized. We define the coverage (θ) of adatoms on silicene as the ratio of the number of adatoms to the number of silicene unit cells. Figure 4 shows the structure models for $\theta = 1$, $\theta = 1/2$, $\theta = 1/3$, and $\theta = 1/4$. Since the nearest neighbor distances in the bulk K and Ca are larger than the lattice constant of the silicene unit cell, we consider only the $\theta = 1/3$ and $1/4$ cases for K and Ca. The E_b, lattice constants, and h for these structures are listed in Table II. The structures with the largest coverage are all stable for Li, Na, K, and Ca on silicene with a larger E_b than E_c. We note that the unit cell of the structures with $\theta = 1/3$ and $1/4$ for the Na, K, and Ca adatoms is a little stretched with respect to the pristine silicene.

B. Groups III and IV metal adatoms

For the Al, Ga, In, and Sn adatoms on silicene, the TA site becomes their favored site, whereas the group III metal (Sn) adatoms on graphene favor the H (bridge) site. Moreover, the E_b of Al, Ga, and In on silicene are almost three times as large as those on graphene. There is hybridization between the adatom sp states and the silicene states around and below

TABLE II. The binding energies (E_b), lattice constants, and heights of the adatoms over the plane of sublattice B defined by the Si atom with largest z (h) for the structures of Li, Na, K, and Ca adatoms on silicene with coverage (θ) larger than or equal to 1/4.

Atom	θ	E_b (eV)	Lattice constant(s) (Å)	h (Å)
Li	1	1.952	3.85	1.43
	1/2	1.991	3.87, 6.69	1.23
	1/3	2.016	6.69	1.43
	1/4	2.034	7.73	1.31
Na	1	1.364	3.87	2.11
	1/2	1.298	3.89, 6.72	1.92
	1/3	1.378	6.73	1.94
	1/4	1.436	7.76	1.84
K	1/3	1.433	6.73	2.39
	1/4	1.541	7.76	2.35
Ca	1/3	2.129	6.72	1.74
	1/4	2.124	7.75	1.66

E_F for Al, Ga, and In on silicene. The bonding is thus mainly covalent for these adatoms on silicene, whereas the bonding between these adatoms and graphene can be characterized to be ionic.[16] Although the Sn adatom binds rather weakly to graphene,[16] strong covalent bonds form between Sn on silicene and its nearest Si atoms, with E_b/E_c reaching 0.935.

When the Al, Ga, In, and Sn atoms are adsorbed at the TA site of silicene, the silicon atom directly below the adatom undergoes a great displacement towards the outside of the plane of sublattice A, as shown in Fig. 5. The large displacement of this Si atom indicates strong bonding between the adatom and the neighboring Si atoms. The M-Si bond lengths ($d_{\text{M-Si}}$) are 2.55, 2.63, 2.95, and 2.75 Å for Al, Ga, In, and Sn, respectively. The E_b/E_c for these adatoms on silicene are larger than 0.830, while the E_b/E_c are smaller than 0.310 for these atoms adsorbed on graphene.[16]

Figure 6 shows the DOS for Al@TA, Al@H, and Sn@TA on silicene. For Al@TA, the Al s state is hybridized with

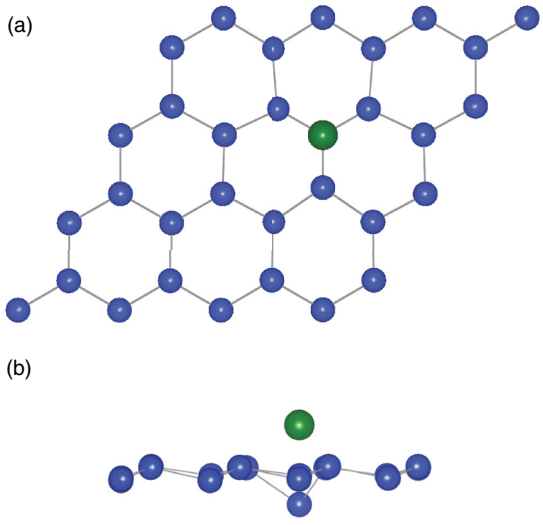

FIG. 5. (Color online) (a) and (b) The relaxed structure for Al@TA on silicene. The larger circle represents the Al atom.

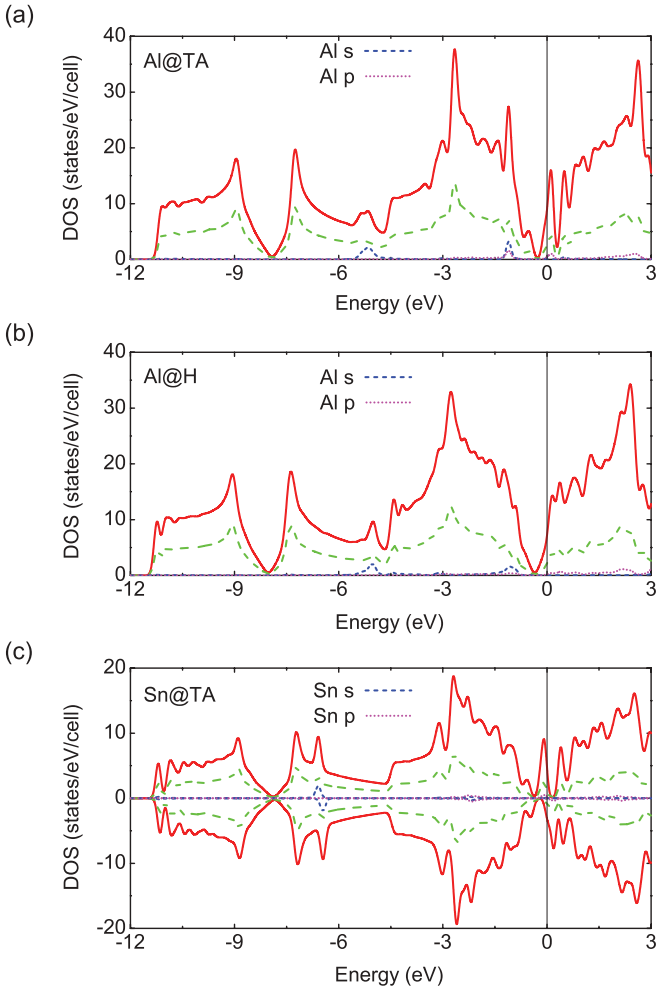

FIG. 6. (Color online) The DOS plots for Al@TA (a), Al@H (b), and Sn@TA (c) on silicene.

the silicene states at the energy 5.6 eV below E_F. And hybridization between the Al sp states and the silicene states occurs at 1.11 eV below E_F. The DOS peak around E_F is mainly contributed by the hybridization states between the Al p states and silicene states. Although rather strong hybridization is present at E_F, the Dirac point is still visible. It is noted that a DOS peak mainly contributed by the silicene states lies 0.5 eV below E_F. This is probably due to the significant deformation of the Si atoms near the Al adatom. For Al@H on silicene, two DOS peaks due to the hybridization between the Al sp states and the silicene states arise below E_F. Similar to Al@H on graphene, the silicene states around the Dirac point are almost unaffected for Al@H on silicene. When the Sn atom is adsorbed at the TA site on silicene, there exists a strong interaction between the Sn p states and the silicene states around E_F. The bonding between Sn and silicene is thus predominately covalent. And the Sn adatom is magnetic with a magnetic moment of 2.00 μ_B.

C. Transition metal adatoms

For adsorption of the Ti, Fe, Co, Ni, Pd, Pt, and Au atoms on silicene, strong covalent bonds form between the adatoms and their nearest Si atoms. All these adatoms bind most strongly

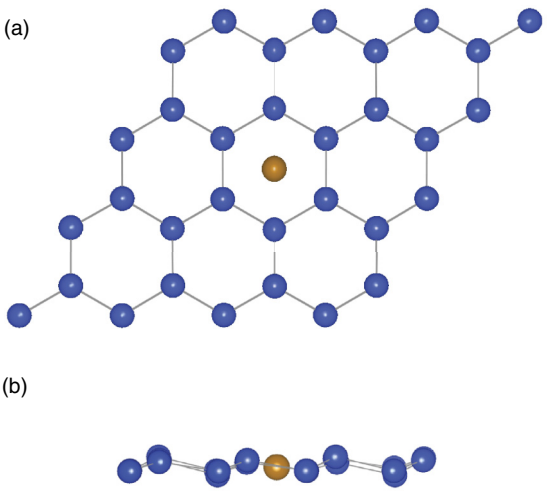

FIG. 7. (Color online) (a) and (b) The relaxed structure for Fe@H on silicene. The light gray circle represents the Fe atom.

to the H site except for Fe, whose favored site is TA. Among these transition metal adatoms, Co, Ni, Pd, and Pt have a larger E_b than E_c. In contrast, the E_b for these adatoms on graphene are all much smaller than E_c with Ni having the largest E_b/E_c of 0.628.[24] The adatom states are strongly hybridized with the silicene states around E_F for Ti@H, Fe@TA, Co@H, and Au@H on silicene. For Ni, Pd, and Pt at the H site of silicene, the DOS peaks resulting from the interaction between the adatom d states and the silicene states lie rather far below the E_F with E_F located approximately at E_D.

The Ti, Co, Ni, Pd, Pt, and Au adatoms on silicene all favor the H site. The E_b are larger than E_c for Co@H, Ni@H, Pd@H, and Pt@H on silicene with rather small h. For Co@H

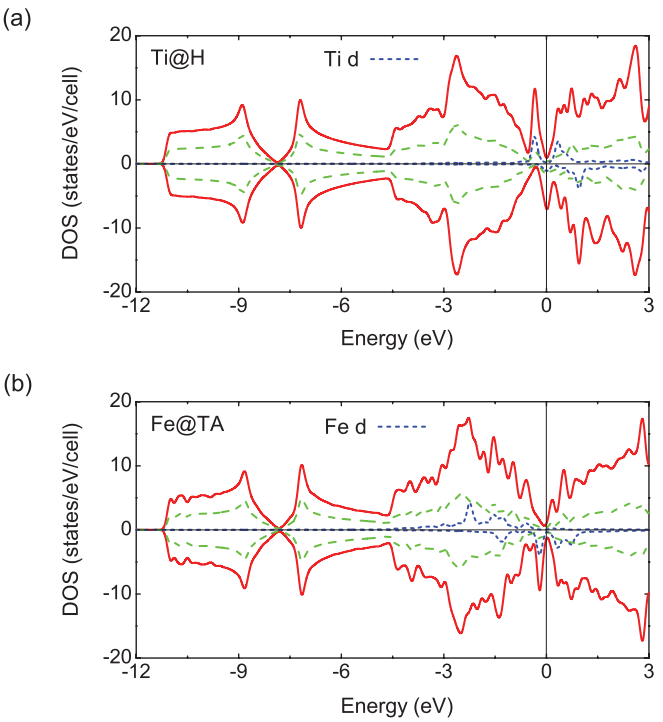

FIG. 8. (Color online) The DOS plots for Ti@H (a) and Fe@TA (b) on silicene.

and Ni@H on silicene, the h are almost equal to each other as well as the $d_{\text{M-Si}}$. The Pt adatom at the H site on silicene has a larger E_b than Pd@H by 1.671 eV, reflected in the structural parameters with Pt having smaller h and $d_{\text{M-Si}}$ than Pd. In addition, we note that the E_b for Au@H reaches 2.316 eV, while the interaction of Au with graphene is rather weak with E_b of only 0.096 eV.[16] In the case of Fe@H on silicene, E_b is a little smaller than E_b at the TA site. Figure 7 shows the peculiar structure of Fe@H. The Fe adatom is adsorbed approximately at the center of a hexagon. The six Fe-Si bonds have almost the same length and are about 2.30 Å, close to the Si-Si bond length (2.39 Å) in silicene. The distortions of both sublattices in the z direction are rather small for Fe@H compared with other transition metal adatoms considered here at the H site. For the Co, Ni, Pd, and Pt adatoms on silicene, the difference between the E_b at the H and TA sites are 0.405, 0.607, 0.499, and 0.623 eV respectively. Using the NEB method, we find that the energy barrier for diffusion of Ni on silicene from the H to the TA site is about 0.749 eV. The calculated diffusion barrier between the neighboring H sites through the top of the Si-Si bond is about 1.560 eV. Therefore, similar to the K adatom on silicene, the favored diffusion path for the Ni adatom on silicene from the H site to the next H site is through the TA site. The much larger diffusion barrier of the Ni adatom on silicene than that of the K adatom on silicene can be attributed to the strong covalent bonds between the Ni adatom and the neighboring Si atoms.

For Ti@H on silicene, the Ti $3d$ states are hybridized with the silicene states mainly around and above E_F for both the spin-up and spin-down states, as shown in Fig. 8(a). The Dirac point is no longer visible. The Ti adatom has a magnetic moment of 2.00 μ_B. The energy splitting between the spin-up and spin-down Ti $3d$ main peaks is about 0.37 eV. For Fe@TA on silicene, three main Fe $3d$ peaks lie below E_F for the spin-up state, as shown in Fig. 8(b). For the spin-down state, only two main Fe $3d$ peaks are occupied. The Fe@TA is magnetic with a magnetic moment of 2.00 μ_B.

In the cases of Fe, Co, and Ni adsorbed at the H site on silicene, Fe and Co are magnetic while Ni is nonmagnetic. Figure 9 shows the DOS for these systems. For Fe@H with a magnetic moment of 1.68 μ_B, the energy splitting between the main Fe $3d$ peaks of spin-up and spin-down states is about 0.57 eV. The E_F lies away from the main Fe $3d$ peak for both spins. Above E_F, interaction between the Fe 3d states and the silicene states is rather weaker for the spin-up state than that for the spin-down state. For adsorption of Co at the H site on silicene, the Dirac point can still be identified. The main Co $3d$ peak lies just below E_F, with E_F below and close to E_D. The Co adatom on silicene has a rather small magnetic moment of

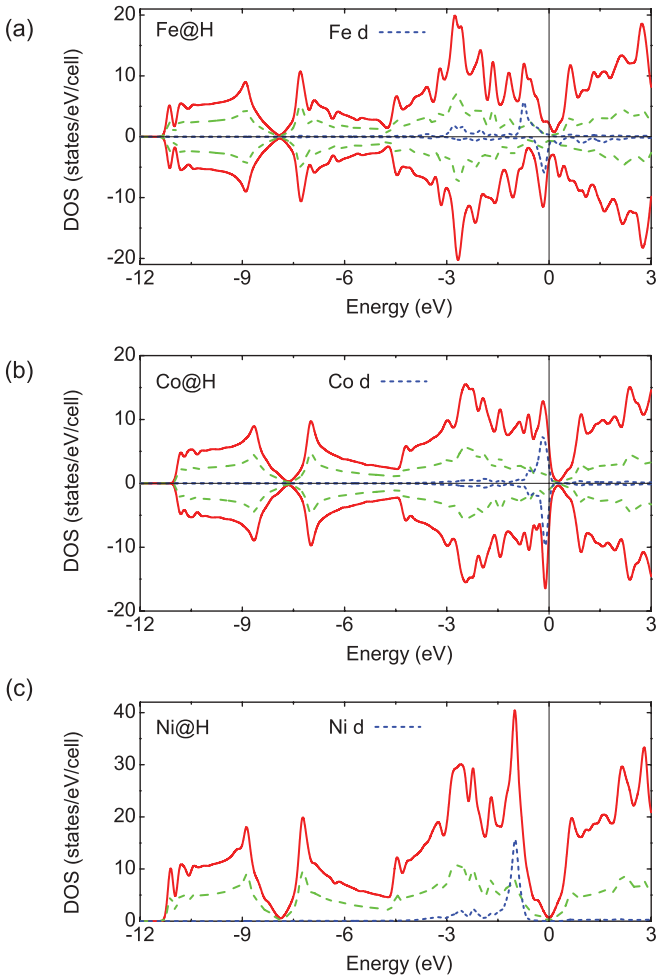

FIG. 9. (Color online) The DOS plots for Fe@H (a), Co@H (b), and Ni@H (c) on silicene.

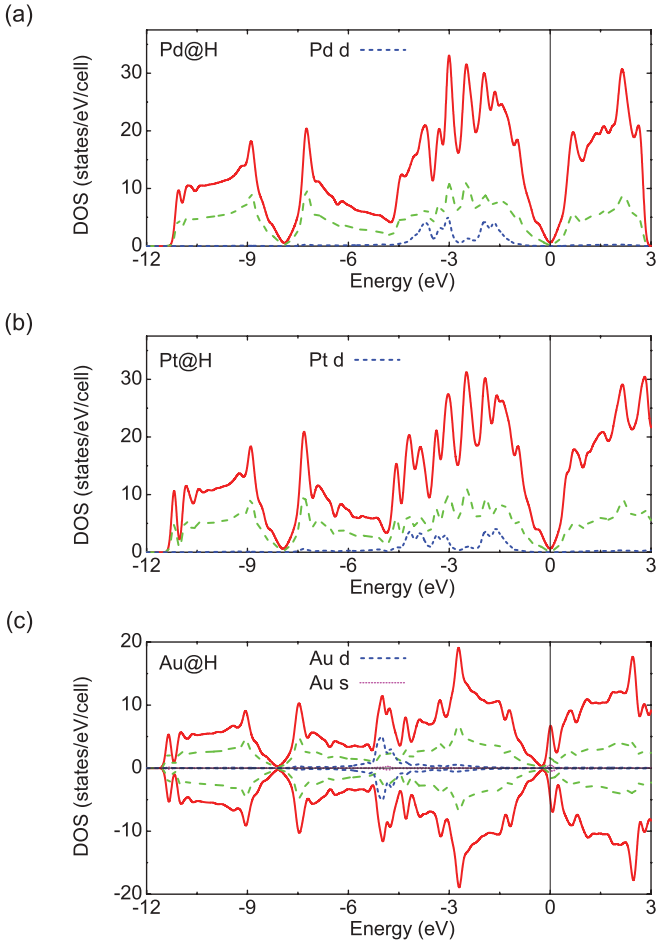

FIG. 10. (Color online) The DOS plots for Pd@H (a), Pt@H (b), and Au@H (c) on silicene.

0.05 μ_B. In contrast, the Co atom adsorbed on graphene has a relatively larger magnetic moment of 1.43 μ_B with E_F located at a Co 3*d* peak.[16] For Ni@H on silicene, the main Ni 3*d* peak lies about 1.00 eV below E_F. The interaction between the Ni 3*d* states and the silicene states is weak around and above E_F. The E_F lies just at E_D.

For silicene adsorbed with Pd and Pt at the H site, the characteristics of the DOS are similar to each other, as shown in Fig. 10. The interaction between the adatom *d* states and the silicene states arise within the energy ranges of $-4.72 \sim -0.88$ eV and $-5.41 \sim -0.80$ eV for Pd and Pt, respectively. Above these energy ranges, there is little interaction between the Pd and Pt states and the silicene states. The E_F are located just at the Dirac point. In contrast, for Pd adsorbed on graphene, a Pd 5*s* peak lies 0.90 eV above E_F and is hybridized with the graphene states.[16] For Au@H, the Au 5*d* states are hybridized with the silicene states below E_F with the main Au 5*d* peak lying at the energy 5.02 eV below E_F. Around E_F, the DOS peak is contributed by the hybridization between the Au 6*s* state and the silicene states. The Au adatom has a magnetic moment of 0.57 μ_B, and the energy splitting due to spin polarization is about 0.08 eV. The Dirac point can still be identified at the energy 0.25 eV below E_F.

IV. SUMMARY

Spin polarized DFT calculations have been performed to study the structural, energetic, and electronic properties of silicene adsorbed with 15 different metal atoms. We find that alkali and alkali-earth metal adatoms Li, Na, K, and Ca and transition metal adatoms Co, Ni, Pd, and Pt obtain a larger E_b than E_c, while for the 15 adatoms considered here on graphene, all the E_b are smaller than E_c. Although the Au and Sn adatoms bind rather weakly to graphene with E_b smaller than 0.260 eV within the GGA, the E_b for Au and Sn on silicene are larger than 2.300 eV. The Li, Na, K, Ca, Ti, Co, Ni, Pd, Pt, and Au adatoms bind most strongly to the H site on silicene. The favored sites of Al, Ga, In, Sn, and Fe on silicene are the TA site. For alkali metal adatoms on silicene, the adatom *s* states lie rather far above E_F. The silicene states remain almost unaltered below the adatom *s* state. The bonding between an alkali metal adatom and silicene is approximately ideal ionic. For the Ca adatom on silicene, besides the charge transfer from Ca to silicene, the hybridization between the Ca 3*d* states and the silicene states around E_F also contributes to the strong binding of Ca to silicene. The Al, Ga, In, and Sn atoms adsorbed on silicene form strong covalent bonds with their nearest Si atoms. When the transition metal atoms considered here are adsorbed on silicene, the adatom *d* states are strongly hybridized with the silicene states. For Ti, Fe, Co, and Au on silicene, the adatom *d* peaks lie around E_F, while they are located rather far below E_F for Ni, Pd, and Pt on silicene with E_F approximately at E_D. The strong binding of metal adatoms to silicene and the rich electronic properties of the systems make it possible to explore experimentally the potential applications in hydrogen storage, superconductivity, and catalysis as well as electronics.

ACKNOWLEDGMENT

This research was supported by the National Natural Science Foundation of China under Grant Nos. 11174171 and 10721404.

*junni@mail.tsinghua.edu.cn

[1] K. S. Novoselov, A. K. Geim, S. V. Morozov, D. Jiang, Y. Zhang, S. V. Dubonos, I. V. Grigorieva, and A. A. Firsov, Science **306**, 666 (2004).
[2] A. K. Geim and K. S. Novoselov, Nat. Mater. **6**, 183 (2007).
[3] A. H. Castro Neto, F. Guinea, N. M. R. Peres, K. S. Novoselov, and A. K. Geim, Rev. Mod. Phys. **81**, 109 (2009).
[4] D. S. L. Abergel, V. Apalkov, J. Berashevich, K. Ziegler, and T. Chakraborty, Adv. Phys. **59**, 261 (2010).
[5] C. N. R. Rao, A. K. Sood, K. S. Subrahmanyam, and A. Govindaraj, Angew. Chem. Int. Ed. **48**, 7752 (2009).
[6] C. Leandri, G. Le Lay, B. Aufray, C. Girardeaux, J. Avila, M. E. Dávila, M. C. Asensio, C. Ottaviani, and A. Cricenti, Surf. Sci. **574**, L9 (2005).
[7] H. Nakano, T. Mitsuoka, M. Harada, K. Horibuchi, H. Nozaki, N. Takahashi, T. Nonaka, Y. Seno, and H. Nakamura, Angew. Chem. **118**, 6451 (2006).
[8] H. Sahaf, L. Masson, C. Léandri, B. Aufray, G. Le Lay, and F. Ronci, Appl. Phys. Lett. **90**, 263110 (2007).
[9] P. De Padova, C. Quaresima, P. Perfetti, B. Olivieri, C. Leandri, B. Aufray, S. Vizzini, and G. Le Lay, Nano Lett. **8**, 271 (2008).
[10] A. Kara, H. Enriquez, A. P. Seitsonen, L. C. Lew Yan Voon, S. Vizzini, B. Aufray, and H. Oughaddou, Surf. Sci. Rep. **67**, 1 (2012).
[11] P. Vogt, P. De Padova, C. Quaresima, J. Avila, E. Frantzeskakis, M. C. Asensio, A. Resta, B. Ealet, and G. Le Lay, Phys. Rev. Lett. **108**, 155501 (2012).
[12] S. Cahangirov, M. Topsakal, E. Aktürk, H. Şahin, and S. Ciraci, Phys. Rev. Lett. **102**, 236804 (2009).
[13] Y. Ding and J. Ni, Appl. Phys. Lett. **95**, 083115 (2009).
[14] S. Lebègue and O. Eriksson, Phys. Rev. B **79**, 115409 (2009).
[15] C.-C. Liu, W. Feng, and Y. Yao, Phys. Rev. Lett. **107**, 076802 (2011).
[16] K. T. Chan, J. B. Neaton, and M. L. Cohen, Phys. Rev. B **77**, 235430 (2008).
[17] G. Profeta, M. Calandra, and F. Mauri, Nat. Phys. **8**, 131 (2012).
[18] I. Cabria, M. J. López, and J. A. Alonso, J. Chem. Phys. **123**, 204721 (2005).
[19] C. Ataca, E. Aktürk, S. Ciraci, and H. Ustunel, Appl. Phys. Lett. **93**, 043123 (2008).
[20] C. Ataca, E. Aktürk, and S. Ciraci, Phys. Rev. B **79**, 041406(R) (2009).
[21] Z. M. Ao and F. M. Peeters, Phys. Rev. B **81**, 205406 (2010).
[22] Y.-H. Lu, M. Zhou, C. Zhang, and Y.-P. Feng, J. Phys. Chem. C **113**, 20156 (2009).
[23] Y. Li, Z. Zhou, G. Yu, W. Chen, and Z. Chen, J. Phys. Chem. C **114**, 6250 (2010).

[24]C. Cao, M. Wu, J. Jiang, and H.-P. Cheng, Phys. Rev. B **81**, 205424 (2010).
[25]O. Ü. Aktürk and M. Tomak, Phys. Rev. B **80**, 085417 (2009).
[26]I. Cabria, M. J. López, and J. A. Alonso, Phys. Rev. B **81**, 035403 (2010).
[27]A. V. Krasheninnikov, P. O. Lehtinen, A. S. Foster, P. Pyykkö, and R. M. Nieminen, Phys. Rev. Lett. **102**, 126807 (2009).
[28]J. A. Rodríguez-Manzo, O. Cretu, and F. Banhart, ACS Nano **4**, 3422 (2010).
[29]X. Yang and J. Ni, Phys. Rev. B **72**, 195426 (2005).
[30]G. Kresse and J. Furthmuller, Comput. Mater. Sci. **6**, 15 (1996); Phys. Rev. B **54**, 11169 (1996).
[31]J. P. Perdew, K. Burke, and M. Ernzerhof, Phys. Rev. Lett. **77**, 3865 (1996).
[32]G. Kresse and D. Joubert, Phys. Rev. B **59**, 1758 (1999).
[33]H. J. Monkhorst and J. D. Pack, Phys. Rev. B **13**, 5188 (1976).
[34]G. Makov and M. C. Payne, Phys. Rev. B **51**, 4014 (1995).
[35]J. Neugebauer and M. Scheffler, Phys. Rev. B **46**, 16067 (1992).
[36]C. Kittel, *Introduction to Solid State Physics*, 8th ed. (Wiley, New York, 2005).
[37]G. Mills, H. Jónsson, and G. K. Schenter, Surf. Sci. **324**, 305 (1995).
[38]M. Caragiu and S. Finberg, J. Phys.: Condens. Matter **17**, R995 (2005).
[39]C.-L. Song, B. Sun, Y.-L. Wang, Y.-P. Jiang, L. Wang, K. He, X. Chen, P. Zhang, X.-C. Ma, and Q.-K. Xue, Phys. Rev. Lett. **108**, 156803 (2012).